Localized hippocampus measures are associated with Alzheimer pathology and cognition independent of total hippocampal volume

Owen Carmichael[1], **Jing Xie**[2], **Evan Fletcher**[1], **Baljeet Singh**[1], **Charles DeCarli**[1], and **the Alzheimer's Disease Neuroimaging Initiative**[*]

[1]Department of Neurology, School of Medicine, University of California, Davis

[2]Graduate Group in Computer Science, School of Engineering, University of California, Davis

Abstract

Hippocampal injury in the Alzheimer's Disease (AD) pathological process is region specific and MRI-based measures of localized hippocampus (HP) atrophy are known to detect region specific changes associated with clinical AD, but it is unclear whether these measures provide information that is independent of that already provided by measures of total HP volume. Therefore, this study assessed the strength of association between localized HP atrophy measures and AD-related measures including CSF amyloid beta and tau concentrations, and cognitive performance, in statistical models that also included total HP volume as a covariate. A computational technique termed localized components analysis (LoCA) was used to identify 7 independent patterns of HP atrophy among 390 semi-automatically delineated HP from baseline MRI of participants in the Alzheimer's Disease Neuroimaging Initiative (ADNI). Among cognitively-normal participants, multiple measures of localized HP atrophy were significantly associated with CSF amyloid concentration, while total HP volume was not. In addition, among all ADNI participants, localized HP atrophy measures and total HP volume were both independently and additively associated with CSF tau concentration, performance on numerous neuropsychological tests, and discrimination between normal, MCI, and AD clinical diagnostic groups. Together, these results suggest that regional measures of hippocampal atrophy provided by LoCA may be more sensitive than total HP volume to the effects of AD pathology burden among cognitively normal individuals and may provide information about HP regions whose deficits may have especially profound cognitive consequences throughout the AD clinical course.

Corresponding author: Owen Carmichael, Center For Neuroscience, 1544 Newton Court, Davis, CA, 95618, Telephone: 530-754-9657, Fax: 530-754-5036.
[*]Data used in the preparation of this article were obtained from the Alzheimer's Disease Neuroimaging Initiative (ADNI) database (www.loni.ucla.edu/ADNI). As such, the investigators within the ADNI contributed to the design and implementation of ADNI and/or provided data but did not participate in analysis or writing of this report. A complete listing of ADNI investigators is available at www.loni.ucla.edu/ADNI/Collaboration/ADNI_Citatation.shtml).

Keywords

Hippocampus; Alzheimer's Disease; morphometry; biomarkers; shape analysis

Introduction

The Alzheimer's Disease (AD) pathological process is hypothesized to begin with the over-production and aggregation of amyloid beta in the brain, followed by the development of neurofibrillary tau pathology in a stereotypical chronological and spatial progression (Hardy and Selkoe, 2002) (Braak and Braak, 1991). According to this schema, neurofibrillary pathology appears first in the transentorhinal region, followed by entorhinal cortex and the CA1 subfield of the hippocampus (HP), finally extending into the CA4 and subiculum HP subfields. It is hypothesized that neurofibrillary pathology in these regions eventually causes neuronal dysfunction and death that leads to impaired memory function, which is the cognitive hallmark of early disease. Measures of medial temporal atrophy from structural magnetic resonance imaging (MRI), including total HP volume, are therefore believed to be sensitive to early AD pathology and the cognitive decline that presumably results from it (Barkhof, et al., 2007,Bobinski, et al., 2000,Bobinski, et al., 1996,Bourgeat, et al., 2010,Csernansky, et al., 2004,deToledo-Morrell, et al., 2007,Gosche, et al., 2002,Jack, et al., 2002,Jagust, et al., 2008,Silbert, et al., 2003,Whitwell, et al., 2008).

Total HP volume, however, is limited in its ability to account for the complex organization of the HP as a collection of functionally interconnected subfields; most investigators combine the contributions of CA1-4, subiculum, dentate gyrus, and possibly other subfields into an overall HP volume measure. Since these regions are damaged differentially by AD-related neurofibrillary pathology, total HP volume may reflect a mix of damaged and healthy subregions early in the AD course.

Partly for this reason, a number of methods for measuring localized HP sub-regions have been developed. Early efforts measured areas of slices oriented perpendicular to the longitudinal HP axis (Laakso, et al., 2000). Another approach measured, at thousands of HP surface points, the "thickness" of the HP in terms of distance from the surface to a central HP axis (Frisoni, et al., 2008). Another method performed high-dimensional warping of HP to a common anatomical template, followed by statistical analysis of the warping using principal components analysis (PCA) (Csernansky, et al., 2005). By relating spatially-variable HP measures to clinical diagnosis of AD, AD risk factors, and other markers, these methods have suggested that a characteristic spatial progression of HP neuronal loss may be detectable *in vivo* from structural MRI (Csernansky, et al., 2005,Laakso, et al., 2000,Morra, et al., 2009,Thompson, et al., 2004,Wang, et al., 2009,Xie, et al., 2009).

These methods for localized HP structure measurement have been limited, however, in their ability to provide measures that integrate HP surface measurements over local neighborhoods, while at the same time being concise and sensitive to AD-related changes. The HP slicing approach loses information about the possibly complex spatial pattern of HP change by collapsing all of the information in an entire slice down to single measurement of surface area. The thickness approach conversely provides the user with thousands of highly localized measurements that do not reduce to a concise set of numbers summarizing broader patterns. The PCA approach does summarize the subject-to-template deformation into a concise set of spatial patterns, but these patterns are not anatomically constrained and therefore typically cover multiple disconnected regions. The biological information contained within each spatial pattern can therefore be difficult to interpret (Alcantara, et al., 2007).

Conversely, Localized Components Analysis (LoCA) provides anatomically constrained information related to structure of the HP (Alcantara, et al., 2007,Alcantara, et al., 2009). Like the PCA approach, it attempts to condense HP shape characteristics into a small number of measurements, each of which describe the structure of a set of HP surface points. Unlike the PCA approach, however, each of the LoCA measurements describes a single, spatially-localized neighborhood. We have previously shown that this method can provide sensitive measurements of biologically-relevant sub-regional changes to a variety of brain structures, including the HP (Harris, et al., 2008,Xie, et al., 2009).

The purpose of this study is to evaluate whether anatomically constrained sub-regional HP shape measurements may add additional information beyond total HP volume to identify aspects of hippocampal structure that are associated with AD pathology and late-life cognitive performance. To accomplish this, we used data from the Alzheimer's Disease Neuroimaging Initiative (www.loni.ucla.edu/ADNI) to relate MRI-based HP measures to CSF-based AD pathology measures, clinical neuropsychological instruments, and clinical diagnosis of MCI and AD. According to the recently described temporal sequence of biomarker changes in AD (Jack, et al., 2010), changes in CSF amyloid precede changes in total HP volume among cognitively-normal individuals possibly by years, and yet pathological studies have shown that HP injury is already occurring among those with abnormal CSF amyloid concentration (Gomez-Isla, et al., 1996) (Braak and Braak, 1991). Because a marker of such mild and early HP damage could play an important role in early detection and quantification of AD pathological effects, we focused on cognitively-normal participants, while additionally extending the analyses to mildly-impaired and demented groups.

Material and methods

Subjects

Data were obtained from the ADNI (www.loni.ucla.edu/ADNI). The ADNI was a 5-year study with a primary goal of testing whether serial MRI, positron emission tomography (PET), other biological markers, and clinical and neuropsychological assessment can be combined to measure the progression of mild cognitive impairment (MCI) and early Alzheimer's disease (AD). Subjects were recruited from over 50 sites across the U.S. and Canada. The initial goal of ADNI was to recruit 800 adults, ages 55 to 90, including approximately 200 cognitively normal older individuals to be followed for 3 years, 400 people with MCI to be followed for 3 years, and 200 people with early AD to be followed for 2 years.

This study includes data from 390 Caucasian ADNI subjects who completed cognitive and clinical evaluations, along with MRI scans, at their baseline visit; 219 of them completed a lumbar puncture for measurement of CSF levels of amyloid and tau. Summary data is shown in Table 1.

Clinical diagnosis and cognitive evaluation

The clinical assessment and cognitive testing of ADNI subjects followed a standardized protocol that was described previously (Petersen, et al., 2010). At each evaluation, all participants underwent a standardized clinical evaluation and cognitive tests. Inclusion criteria for the normal group included MMSE scores between 24 and 30, a Clinical Dementia Rating Scale (CDR) sum of boxes score of 0, and no evidence of major depression, MCI, or dementia. Participants were included in the MCI group if they had a subjective memory complaint, objective memory loss measured by education-adjusted Wechsler Memory Scale-Revised Logical Memory II scores, a CDR Sum of 0.5, absence of

significant impairment in other cognitive domains, preserved activities of daily living, and an absence of dementia. AD participants met the National Institute of Neurological and Communicative Disorders and Stroke and Alzheimer's Disease and Related Disorders Association (NINCDS/ADRDA) criteria for probable AD, had an MMSE between 18 and 26, and a CDR Sum of 0.5 to 1.0. Exclusion criteria included history of structural brain lesions or head trauma, significant neurological disease other than incipient Alzheimer's disease, use of psychotropic medications that could affect memory, and a Hachinski Ischemic Scale score of 4 or greater. MRI findings that served as exclusionary criteria included major hemispheric infarction, or structural abnormalities that severely distort normal brain anatomy such as tumor or prior resective surgery.

Magnetic resonance imaging

Acquisition of 1.5T MRI data at each performance site followed a previously-described standardized protocol that was rigorously validated across sites (Jack, et al., 2008). The protocol included a high-resolution T1-weighted sagittal volumetric magnetization prepared rapid gradient echo (MP-RAGE) sequence. The ADNI MRI core optimized the acquisition parameters of these sequences for each make and model of scanner included in the study. Before being allowed to scan ADNI participants, all performance sites were required to pass a strict scanner validation test, including MP-RAGE scans of human subjects and a spherical fluid-filled phantom. Additionally, each scan of ADNI participants included a scan of the phantom, which was required to pass strict validation tests. All vetted raw scan data was transferred to the University of California, San Francisco for semi-automated HP volumetry.

HP delineation

Semi-automated HP volumetry was carried out using a commercially available high dimensional brain mapping tool (Medtronic Surgical Navigation Technologies, Louisville, CO), that has previously been validated and compared to manual tracing of the HP (Hsu, et al., 2002). Measurement of HP volume is achieved first by placing manually 22 control points as local landmarks for the HP on the individual brain MRI data: one landmark at the HP head, one at the tail, and four per image (i.e., at the superior, inferior, medial and lateral boundaries) on five equally spaced images perpendicular to the long axis of the HP. Second, fluid image transformation is used to match the individual brains to a template brain (Christensen, et al., 1997). The fluid transformation is used to label HP pixels in the native space of the subject scan, resulting in a binary image representation of the HP structure. The number of HP voxels in this space is counted to obtain the total HP volume. This method of measuring HP volume agrees strongly with fully-manual delineations, with a documented intraclass correlation coefficient between semi-automated and manual volumes of .94 (Hsu, et al., 2002). Binary images for each HP were uploaded to the ADNI database at the UCLA Laboratory for Neuroimaging (LONI) and transferred to the UC Davis Imaging of Dementia and Aging Laboratory (IDeA Lab) for further analysis.

Localized components analysis

Each HP ROI mask was converted to a 3D geometric mesh representation, and Localized Components Analysis (LoCA) was used to quantify localized HP deficits (Alcantara, et al., 2007,Alcantara, et al., 2009,Xie, et al., 2009). We first created one-to-one correspondences between subjects at 300 homologous HP surface points using a radial surface mapping approach (Thompson, et al., 2004). Briefly, medial curves were threaded down the central anterior-posterior axis of each HP. For each HP, 15 HP slices were then generated by intersecting the HP with 15 planes that cut the HP perpendicular to the medial curve. Within each slice, rays were then cast along a set of 20 evenly spaced outward directions from the medial curve toward the HP surface. Correspondences were then established across HP between cast rays that had analogous slice position and casting direction, and HP surface

points at which corresponding rays intersected the surface were assumed to be in correspondence. The resulting HP surfaces, each containing the 300 corresponding surface points, were then globally aligned to a common space using Generalized Procrustes Alignment (Gower, 1975). Principal components analysis (PCA) was then applied to the set of aligned HP, resulting in a set of shape components: each shape component can be interpreted as a mode of deformation that linearly deforms the population mean HP. Once a set of shape components are determined, each subject HP can be described by a set of shape component coefficients: these quantify the degrees to which each of the shape component deformations must be applied to the population mean HP to produce an HP shape that matches that of the subject. The LoCA method iteratively modifies the PCA shape components to force each one to cover a spatially-localized HP sub-region, while simultaneously trying to obtain the best fit of all subject HP using the smallest number of shape component deformations possible. The result is a small set of shape components, each of which represents a prominent mode of localized HP shape variability across the population (Xie, Alcantara et al. 2009). Coefficients for the shape components that accounted for at least 3% of HP shape variability were analyzed.

Biomarker measurement

CSF samples were obtained by the individual centers, then banked and batch-processed using a standardized protocol, under the direction of Drs. Leslie Shaw and John Trojanowski of the ADNI Biomarker Core at the University of Pennsylvania School of Medicine (Shaw, 2008). CSF measures at baseline included amyloid β_{1-42} and total tau protein as previously described (Shaw, et al., 2009).

Statistical analysis

For each LoCA shape component, general linear models were constructed that used that shape component's coefficients, total HP volume, age, and gender as simultaneous predictor variables. For each such shape component, separate models were estimated that had CSF measures of amyloid and tau, clinical neuropsychological test instrument scores (see Table 3 for list) and clinical diagnosis (normal *vs.* MCI *vs.* AD) as outcome variables. For each fitted model, the independent effect of the LoCA coefficient was assessed, and this was compared to the effect of HP volume in a model lacking LoCA variables, to assess the relative strengths of association between the outcome measure, and total HP volume and localized HP atrophy respectively.

Among neuropsychological instruments, scores for clock drawing, cube copying, digit spans forward and backward, MMSE, Boston naming, CDR sum of boxes, and delayed story recall had skewed distributions across the population of subjects who received an MRI. Therefore, the scores on these tests were treated as integer values, and Poisson regression was used to determine whether predictor values were associated with a greater or smaller number of test points (CDR sum of boxes scores were re-scaled to account for the presence of 0.5 and 1.5 scores). Scores on the remaining test instruments, as well as the CSF measures of tau and amyloid, were reasonably normally distributed, so linear regression was used to relate predictor variables to outcome variables.

We fitted separate models among those clinically diagnosed as cognitively normal at baseline, those diagnosed with MCI at baseline, and those diagnosed with AD at baseline. Then, for comparison, we fitted combined models including individuals across all three baseline diagnostic categories.

Finally, logistic regression models were used to determine the degree to which the predictor variables increased or decreased the probability of being diagnosed as MCI at baseline,

compared to cognitively normal; and the degree to which the predictors increased or decreased the probability of being diagnosed as AD at baseline, compared to MCI. These models were estimated across the entire population of individuals who received an MRI.

In each of these models, appropriate statistical tests were used to assess the independent predictive power contributed by each of the predictors. To correct for multiple comparisons, we ran permutations tests with 1000 permutations on each fitted statistical model, and report the *p* values for these permutation tests (Werft and Benner, 2010). Whenever there was a significant effect of total HP volume on an outcome variable, we report the number of units difference in the outcome measure that was associated with a. 1 cc difference in total HP volume. Linear change in each local HP atrophy measurement was associated with a linear change in the local HP *thickness*: that is, the distance between the central HP axis and the HP surface point that atrophied the most severely in response to a change in this measurement. Whenever there was a significant effect of a local atrophy measurement on an outcome variable, we report the number of units difference in the outcome measure that was associated with a 1 mm difference in local HP thickness.

Results

General characteristics of all study participants are shown in Table 1. The sub-group of individuals who received both MRI and CSF measurements was broadly similar to the overall sample of those who received an MRI. As expected, the groups indicate stepwise differences in cognitive measures, HP volume, tau pathology, and CSF amyloid beta, with those in the MCI group displaying higher pathology burden and cognitive impairment compared to the normal group, and the AD group displaying higher pathology burden and cognitive impairment compared to the MCI group. However, the difference in CSF amyloid beta burden between MCI and AD groups was not statistically significant.

Seven independent measures of regional HP atrophy, each of which accounted for greater than 3% of HP structural variability across the population, were derived from our LoCA method. Together, the measures accounted for 46% of the variability in HP surface point positions across the cohort. These 7 measures summarized atrophy to the anterior and posterior portions of the inferior head, the superior portion of the medial head and superior, inferior, and lateral portions of the body (Figure 1). Of the two measures accounting for atrophy to the lateral body, the first represented focal deficits to only a limited portion of the lateral body, along with slight deformation of the posterior aspect of the body in the superior-inferior direction. The second represented substantial atrophy to a broader extent of the lateral body, along with lesser degrees of reduction to the superior, medial, and inferior aspects of the tail. These measures accounted for 11.5%, 7.9%, 7.5%, 6.9%, 4.6%, 4.2%, 3.2% of hippocampus variability respectively. The magnitudes of Pearson correlations between pairs of the measures were all less than .3. The magnitudes of Pearson correlations between HP volume and the measures summarizing atrophy to the inferior head regions were less than .5, and all other correlations between HP volume and LoCA measures were less than .25. Therefore we concluded that the LoCA measures and total HP volume were not entirely redundant with each other.

Associations between LoCA and CSF Measures

The association between HP volume and CSF measures of amyloid beta and tau were highly significant when all subjects were included in the same model. Repeated analyses restricted to individual diagnostic categories, however, revealed that HP volume was not significantly associated with either variable within any diagnostic category.

Conversely, LoCA measures that quantified atrophy to the inferior-anterior HP head and the superior and inferior body were significantly associated with a CSF measure of total amyloid beta 1-42 among cognitively normal individuals (Table 2). In these models, each millimeter decrease in local HP thickness was associated with an amyloid beta decrease between 9.9 and 12.4 *pg/ml*. In addition, the LoCA measure of atrophy to the superior body was also significantly related to CSF amyloid burden among individuals diagnosed with MCI at baseline, but no LoCA measure was associated with CSF amyloid burden among those diagnosed with AD at baseline. In the MCI model, a 1 mm decrease in local superior HP body thickness was associated with a 6.18 *pg/ml* decrease in CSF amyloid concentration. In each such model relating LoCA measures to CSF amyloid burden, HP volume was an independent predictor that was not statistically significant. No LoCA atrophy measure was significantly associated with total tau burden in any model that was restricted to one of the three baseline diagnostic groups individually. Similar to total hippocampal volume, however, in a model containing individuals from all three groups together, a significant association between CSF tau and a LoCA measure of the superior HP body was observed (p=0.012). HP volume remained a statistically significant independent predictor in this model (p<.001). In this model, a .1 *cc* decrease in total HP volume was associated with a 3.37 *pg/ml* increase in CSF tau, and a 1 *mm* decrease in local superior HP body thickness was associated with a 4.1 *pg/ml* increase in CSF tau.

Figures 2, 3, and 4 provide renderings of the degree of local HP deformation that corresponds to hypothetical participants with varying levels of amyloid and tau. For Figure 2, we considered a hypothetical male participant in the cognitively normal group whose age (77.0) and total HP volume (2.1 *cc*) were exactly at the cognitively normal average. Given a prescribed level of amyloid burden, we determined the degree of local HP deformation that is required by the statistical model in combination with the provided age, gender, and total HP volume to predict that level of amyloid burden. We then deformed the population mean HP by the requisite degree of local deformation to generate the rendering. The renderings show the local HP deformations corresponding to the median, first quartile, and third quartile of amyloid values among the normal group. The renderings suggest an increasing degree of atrophy to the medial HP head and body as one moves from right to left in the figure, corresponding to increasing amyloid burden (*i.e.*, decreasing concentration of amyloid in the CSF). For Figure 3, we generated analogous renderings showing the local HP deformation for a hypothetical average male MCI participant associated with amyloid levels at the MCI median, first quartile, and third quartile. The renderings suggest that in this group, a focal deficit to the medial HP body is associated with increasing amyloid burden (moving from right to left in the figure). For Figure 4 we show the local HP deformation for a hypothetical average participant from the overall sample whose tau burden is at levels corresponding to the mean values of the normal, MCI, and AD groups. The renderings suggest progressive deficits to the medial body in association with increasing levels of tau burden corresponding to typical normal, MCI, and AD levels.

Correlations between LoCA measures and Cognitive Performance

In addition, three LoCA measures were strongly associated with cognitive function across the entire cohort as measured by a battery of standardized neuropsychological test instruments (Table 3), in models that simultaneously adjusted for total HP volume. In these models, total HP volume was also independently associated with performance. The magnitudes of effect of .1 *cc* difference in total HP volume and 1 *mm* difference in local HP thickness were similar in these models; for example, a .1 *cc* decrease in total HP volume was associated with a 1.3 point increase in ADAS-Cog total score, while 1 *mm* decrease in local HP thickness in the superior, lateral, and inferior body were independently associated with ADAS-Cog total score increases of .79,.73, and 1.0 points. Analysis of either total

hippocampal volume or the LoCA measures did not show significant associations with cognition when subjects within each diagnostic category were examined separately.

Diagnostic Group Differences in LoCA Measures

In a logistic regression model that also included total HP volume, LoCA measures of atrophy to the superior and lateral body significantly discriminated individuals who were cognitively normal at baseline from those who were MCI at baseline ($p=<0.001$ and $p=.033$). In a second model that also included total HP volume, measures of atrophy to the superior and lateral body discriminated those who were diagnosed with MCI at baseline from those diagnosed with AD at baseline ($p=0.021$ and $p=0.043$). In these models, total HP volume was also a significant and independent discriminator between the clinical diagnostic groups ($p<.001$ and $p<.001$). A decrease of .1 *cc* in total HP volume was associated with an increase of 1.19 in the odds of receiving a clinical diagnosis of AD relative to MCI. Decreases of 1 *mm* in local superior body and lateral body thickness were independently associated with increases of 1.19 and 1.22 in odds of diagnosis of AD compared to MCI. A decrease of .1 *cc* in total HP volume was associated with an increase of 1.41 in the odds of receiving a diagnosis of MCI relative to a lack of clinical diagnosis of either MCI or AD. Decreases of 1 *mm* in local superior body and lateral body thickness were independently associated with increases of 1.32 and 1.32 in odds of diagnosis of MCI relative to a lack of clinical diagnosis of either MCI or AD.

Discussion

The first key finding of this study is that LoCA measures of regional HP atrophy may add significant additional information to the understanding of associations between HP atrophy and CSF measures of AD pathology. In particular, we show that LoCA measures may be sensitive to early macroscopic HP changes in the AD cascade by identifying significant associations between LoCA measures and CSF amyloid concentration among cognitively normal individuals, while analogous associations were not found with total HP volume. In light of growing evidence for a temporal sequence of biomarker changes that mark the progression of the AD pathological cascade, this finding supports the notion that our localized HP measures may detect HP subregions particularly vulnerable to AD pathology early in the pathological course of the disease (Gomez-Isla, et al., 1996). According to the amyloid cascade hypothesis, *in vivo* markers of amyloid beta, tau, neuronal death, and cognitive function are believed to become sequentially abnormal in response to a cascade of biochemical events initiated by excessive brain amyloid beta production and accumulation (Jack, et al., 2010) (Hardy and Selkoe, 2002). In this schema, an increase in amyloid burden precedes the release of tau into the CSF and atrophy to medial temporal structures before clinically significant cognitive decline is evident (Sluimer, et al., 2008). Because HP atrophy is known to follow a characteristic spatial pattern during this pathological progression, it is plausible that changes in localized HP measures may precede changes in total HP volume as HP injury follows amyloid and tau accumulation. The finding that our LoCA measures of regional HP atrophy were associated with CSF amyloid concentration among cognitively-normal individuals, while total HP volume was not, supports this notion and therefore suggests that LoCA may be sensitive to the earliest phase of the amyloid cascade. Localized HP measures may thus be useful in imaging studies that probe the earliest stages of AD-related brain changes.

The localized HP measures were significantly associated with CSF amyloid, but not CSF tau, in the cognitively normal group, suggesting that the LoCA measures may be sensitive to HP injury in the AD cascade that is not directly mediated by tau pathology. The reduced dendritic arborization and spine counts observed in HP sub-regions in pathologically-confirmed AD may account for such HP injury (Falke, et al., 2003,Ferrer and Gullotta,

1990). Reports of dendritic spine loss or altered dendritic morphology in the HP of AD transgenic mice that overproduce amyloid, yet generally do not accumulate tau, support the hypothesis that tau accumulation is not a prerequisite for such dendritic injury (Knafo, et al., 2009,Wu, et al., 2004). Given these reports, we speculate that our HP measures may have been associated with amyloid concentration among the cognitively normal group due to HP injury not directly due to tau pathology, such as degeneration of dendritic processes, while the LoCA measures did not associate with tau in this group because tau levels had largely not yet risen to abnormal levels in these individuals. The LoCA measures associated significantly with CSF tau burden across the entire cohort, supporting the notion that tau changes impacting macroscopic HP structure may occur relatively later in the pathological progression. Confirmatory studies, however, will be needed to show how sensitive LoCA measures are to the earliest HP changes related to AD brain pathology.

The second key finding of the study is that localized HP atrophy measures were significantly associated with a CSF-based measure of tau pathology burden, performance on an array of clinical neuropsychological instruments, and discrimination between clinical diagnostic groups, even after controlling for total HP volume. Again following the hypothesized chronology of changes to markers of amyloid, tau, neuronal death, and cognition, this finding may suggest that even after the accumulation of amyloid and tau have led to pronounced HP neuronal death and markedly reduced HP volume, the localized atrophy measures continue to provide independent information about the spatial pattern of HP losses associated with tau accumulation. Significant associations between LoCA measures and cognition suggest that MRI measures of hippocampal subregions may be more specifically associated with the cognitive systems affected by AD pathology. Indeed, the LoCA measure associated with tau appears to correlate with elements of both CA1 and subiculum (Frisoni, et al., 2008), HP regions known to be affected early in the AD process. This LoCA measure is also strongly associated with cognition, even after correcting for total hippocampal atrophy, suggesting that deficits in specific sub-regions may have especially profound cognitive consequences. This finding underscores the importance of understanding the functional organization of the HP as a network of distinct subunits that contribute differentially to common cognitive tasks (Amaral, 1993). On a practical level, this finding suggests that localized HP measures may provide value above and beyond that already provided by HP volume for modeling the effects of AD pathology on the brain and cognition.

The key limitation of the study is the lack of multiple measurements of amyloid, tau, HP structure, and cognition per individual over time. Lacking these measurements, this study used cross-sectional measurements together with the hypothesized temporal sequence of AD-related changes to draw inferences about relationships between changes in HP measures and longitudinal changes in amyloid, tau, and cognition. Further establishing the utility of the localized HP measures as early AD markers requires analysis of relationships between longitudinal HP change measures, based on multiple MRI scans per individual and longitudinal changes in the other markers. The raw longitudinal data for this analysis is available from ADNI, but a longitudinal analog of LoCA needs to be developed; that is, a method for concise measurement of per-individual longitudinal changes to localized HP regions over time based on multiple MRI scans. Future work should involve development of such a method and application to longitudinal data such as that provided by ADNI.

Another important limitation is the lack of ethnic diversity among participants. This study excluded the small number of ADNI participants from non-Caucasian ethnic groups due to their heterogeneity and the confounding effects ethnicity may have on brain structure. However, accumulating evidence suggests that the natural history of structural and cognitive changes leading to dementia may differ between ethnic groups (Brickman, et al., 2008)

(DeCarli, et al., 2008) (Stavitsky, et al., 2010). While an earlier study suggested that LoCA is able to identify biologically plausible relationships between hippocampal and cognitive changes suggestive of clinical AD in an ethnically-diverse cohort (Xie, et al., 2009), the current findings relating AD pathology burden to LoCA measures need to be replicated in an ethnically diverse cohort to clarify their generalizability.

Acknowledgments

References

Alcantara D, Carmichael O, Delson E, Harcourt-Smith W, Sterner K, Frost S, Dutton R, Thompson P, Aizenstein H, Lopez O, Becker J, Amenta N. Localized components analysis. Inf Process Med Imaging. 2007; 20:519–31. [PubMed: 17633726]

Alcantara DA, Carmichael O, Harcourt-Smith W, Sterner K, Frost SR, Dutton R, Thompson P, Delson E, Amenta N. Exploration of shape variation using localized components analysis. IEEE Trans Pattern Anal Mach Intell. 2009; 31(8):1510–6. 10.1109/TPAMI.2008.287 [doi]. [PubMed: 19542583]

Amaral DG. Emerging principles of intrinsic hippocampal organization. Curr Opin Neurobiol. 1993; 3(2):225–9. [PubMed: 8390320]

Barkhof F, Polvikoski TM, van Straaten EC, Kalaria RN, Sulkava R, Aronen HJ, Niinisto L, Rastas S, Oinas M, Scheltens P, Erkinjuntti T. The significance of medial temporal lobe atrophy: a postmortem MRI study in the very old. Neurology. 2007; 69(15):1521–7. 69/15/1521 [pii] 10.1212/01.wnl.0000277459.83543.99 [doi]. [PubMed: 17923614]

Bobinski M, de Leon MJ, Wegiel J, Desanti S, Convit A, Saint Louis LA, Rusinek H, Wisniewski HM. The histological validation of post mortem magnetic resonance imaging-determined hippocampal volume in Alzheimer's disease. Neuroscience. 2000; 95(3):721–5. [PubMed: 10670438]

Bobinski M, Wegiel J, Wisniewski HM, Tarnawski M, Reisberg B, De Leon MJ, Miller DC. Neurofibrillary pathology--correlation with hippocampal formation atrophy in Alzheimer disease. Neurobiol Aging. 1996; 17(6):909–19. S0197458096001601 [pii]. [PubMed: 9363803]

Bourgeat P, Chetelat G, Villemagne VL, Fripp J, Raniga P, Pike K, Acosta O, Szoeke C, Ourselin S, Ames D, Ellis KA, Martins RN, Masters CL, Rowe CC, Salvado O, Group AR. Beta-amyloid burden in the temporal neocortex is related to hippocampal atrophy in elderly subjects without dementia. Neurology. 2010; 74(2):121–7. 74/2/121 [pii] 10.1212/WNL.0b013e3181c918b5 [doi]. [PubMed: 20065247]

Braak H, Braak E. Neuropathological stageing of Alzheimer-related changes. Acta Neuropathol. 1991; 82(4):239–59. [PubMed: 1759558]

Brickman AM, Schupf N, Manly JJ, Luchsinger JA, Andrews H, Tang MX, Reitz C, Small SA, Mayeux R, DeCarli C, Brown TR. Brain morphology in older African Americans, Caribbean Hispanics, and whites from northern Manhattan. Arch Neurol. 2008; 65(8):1053–61. 65/8/1053 [pii] 10.1001/archneur.65.8.1053 [doi]. [PubMed: 18695055]

Christensen GE, Joshi SC, Miller MI. Volumetric transformation of brain anatomy. IEEE Trans Med Imaging. 1997; 16(6):864–77. 10.1109/42.650882 [doi]. [PubMed: 9533586]

Csernansky JG, Hamstra J, Wang L, McKeel D, Price JL, Gado M, Morris JC. Correlations between antemortem hippocampal volume and postmortem neuropathology in AD subjects. Alzheimer Dis Assoc Disord. 2004; 18(4):190–5. 00002093-200410000-00006 [pii]. [PubMed: 15592129]

Csernansky JG, Wang L, Swank J, Miller JP, Gado M, McKeel D, Miller MI, Morris JC. Preclinical detection of Alzheimer's disease: hippocampal shape and volume predict dementia onset in the elderly. Neuroimage. 2005; 25(3):783–92. S1053-8119(04)00785-2 [pii] 10.1016/j.neuroimage. 2004.12.036 [doi]. [PubMed: 15808979]

DeCarli C, Reed BR, Jagust W, Martinez O, Ortega M, Mungas D. Brain behavior relationships among African Americans, whites, and Hispanics. Alzheimer Dis Assoc Disord. 2008; 22(4):382–91. [PubMed: 19068502]

deToledo-Morrell L, Stoub TR, Wang C. Hippocampal atrophy and disconnection in incipient and mild Alzheimer's disease. Prog Brain Res. 2007; 163:741–53. S0079- 6123(07)63040-4 [pii] 10.1016/S0079-6123(07)63040-4 [doi]. [PubMed: 17765748]

Falke E, Nissanov J, Mitchell TW, Bennett DA, Trojanowski JQ, Arnold SE. Subicular dendritic arborization in Alzheimer's disease correlates with neurofibrillary tangle density. Am J Pathol. 2003; 163(4):1615–21. [PubMed: 14507668]

Ferrer I, Gullotta F. Down's syndrome and Alzheimer's disease: dendritic spine counts in the hippocampus. Acta Neuropathol. 1990; 79(6):680–5. [PubMed: 2141748]

Frisoni GB, Ganzola R, Canu E, Rub U, Pizzini FB, Alessandrini F, Zoccatelli G, Beltramello A, Caltagirone C, Thompson PM. Mapping local hippocampal changes in Alzheimer's disease and normal ageing with MRI at 3 Tesla. Brain. 2008; 131(Pt 12):3266–76. awn280 [pii] 10.1093/brain/awn280 [doi]. [PubMed: 18988639]

Gomez-Isla T, Price JL, McKeel DW Jr, Morris JC, Growdon JH, Hyman BT. Profound loss of layer II entorhinal cortex neurons occurs in very mild Alzheimer's disease. J Neurosci. 1996; 16(14): 4491–500. [PubMed: 8699259]

Gosche KM, Mortimer JA, Smith CD, Markesbery WR, Snowdon DA. Hippocampal volume as an index of Alzheimer neuropathology: findings from the Nun Study. Neurology. 2002; 58(10):1476–82. [PubMed: 12034782]

Gower J. Generalized procrustes analysis. Psychometrika. 1975; 40(1):33–51.10.1007/bf02291478

Hardy J, Selkoe DJ. The amyloid hypothesis of Alzheimer's disease: progress and problems on the road to therapeutics. Science. 2002; 297(5580):353–6. 10.1126/science.1072994 [doi] 297/5580/353 [pii]. [PubMed: 12130773]

Harris P, Alcantara DA, Amenta N, Lopez OL, Eiriksdottir G, Sigurdsson S, Gudnason V, Madsen S, Thompson PM, Launer LJ, Carmichael OT. Localized measures of callosal atrophy are associated with late-life hypertension: AGES-Reykjavik Study. Neuroimage. 2008; 43(3):489–96. S1053-8119(08)00800-8 [pii] 10.1016/j.neuroimage.2008.07.007 [doi]. [PubMed: 18692143]

Hsu YY, Schuff N, Du AT, Mark K, Zhu X, Hardin D, Weiner MW. Comparison of automated and manual MRI volumetry of hippocampus in normal aging and dementia. J Magn Reson Imaging. 2002; 16(3):305–10. 10.1002/jmri.10163 [doi]. [PubMed: 12205587]

Jack CR Jr, Bernstein MA, Fox NC, Thompson P, Alexander G, Harvey D, Borowski B, Britson PJ, J LW, Ward C, Dale AM, Felmlee JP, Gunter JL, Hill DL, Killiany R, Schuff N, Fox-Bosetti S, Lin C, Studholme C, DeCarli CS, Krueger G, Ward HA, Metzger GJ, Scott KT, Mallozzi R, Blezek D, Levy J, Debbins JP, Fleisher AS, Albert M, Green R, Bartzokis G, Glover G, Mugler J, Weiner MW. The Alzheimer's Disease Neuroimaging Initiative (ADNI): MRI methods. J Magn Reson Imaging. 2008; 27(4):685–91. [PubMed: 18302232]

Jack CR Jr, Dickson DW, Parisi JE, Xu YC, Cha RH, O'Brien PC, Edland SD, Smith GE, Boeve BF, Tangalos EG, Kokmen E, Petersen RC. Antemortem MRI findings correlate with hippocampal neuropathology in typical aging and dementia. Neurology. 2002; 58(5):750–7. [PubMed: 11889239]

Jack CR Jr, Knopman DS, Jagust WJ, Shaw LM, Aisen PS, Weiner MW, Petersen RC, Trojanowski JQ. Hypothetical model of dynamic biomarkers of the Alzheimer's pathological cascade. Lancet Neurol. 2010; 9(1):119–28. [PubMed: 20083042]

Jagust WJ, Zheng L, Harvey DJ, Mack WJ, Vinters HV, Weiner MW, Ellis WG, Zarow C, Mungas D, Reed BR, Kramer JH, Schuff N, DeCarli C, Chui HC. Neuropathological basis of magnetic resonance images in aging and dementia. Ann Neurol. 2008; 63(1):72–80. [PubMed: 18157909]

Knafo S, Alonso-Nanclares L, Gonzalez-Soriano J, Merino-Serrais P, Fernaud-Espinosa I, Ferrer I, DeFelipe J. Widespread changes in dendritic spines in a model of Alzheimer's disease. Cereb Cortex. 2009; 19(3):586–92. bhn111 [pii] 10.1093/cercor/bhn111. [PubMed: 18632740]

Laakso MP, Frisoni GB, Kononen M, Mikkonen M, Beltramello A, Geroldi C, Bianchetti A, Trabucchi M, Soininen H, Aronen HJ. Hippocampus and entorhinal cortex in frontotemporal dementia and Alzheimer's disease: a morphometric MRI study. Biol Psychiatry. 2000; 47(12): 1056–63. S0006322399003066 [pii]. [PubMed: 10862805]

Morra JH, Tu Z, Apostolova LG, Green AE, Avedissian C, Madsen SK, Parikshak N, Hua X, Toga AW, Jack CR Jr, Schuff N, Weiner MW, Thompson PM. Automated 3D mapping of hippocampal atrophy and its clinical correlates in 400 subjects with Alzheimer's disease, mild cognitive impairment, and elderly controls. Hum Brain Mapp. 2009; 30(9):2766–88. 10.1002/hbm.20708 [doi]. [PubMed: 19172649]

Petersen RC, Aisen PS, Beckett LA, Donohue MC, Gamst AC, Harvey DJ, Jack CR Jr, Jagust WJ, Shaw LM, Toga AW, Trojanowski JQ, Weiner MW. Alzheimer's Disease Neuroimaging Initiative (ADNI): clinical characterization. Neurology. 2010; 74(3):201–9. WNL.0b013e3181cb3e25 [pii] 10.1212/WNL.0b013e3181cb3e25. [PubMed: 20042704]

Shaw LM. PENN biomarker core of the Alzheimer's disease Neuroimaging Initiative. Neurosignals. 2008; 16(1):19–23. 000109755 [pii] 10.1159/000109755 [doi]. [PubMed: 18097156]

Shaw LM, Vanderstichele H, Knapik-Czajka M, Clark CM, Aisen PS, Petersen RC, Blennow K, Soares H, Simon A, Lewczuk P, Dean R, Siemers E, Potter W, Lee VM, Trojanowski JQ. Cerebrospinal fluid biomarker signature in Alzheimer's disease neuroimaging initiative subjects. Ann Neurol. 2009; 65(4):403–13. 10.1002/ana.21610 [doi]. [PubMed: 19296504]

Silbert LC, Quinn JF, Moore MM, Corbridge E, Ball MJ, Murdoch G, Sexton G, Kaye JA. Changes in premorbid brain volume predict Alzheimer's disease pathology. Neurology. 2003; 61(4):487–92. [PubMed: 12939422]

Sluimer JD, van der Flier WM, Karas GB, Fox NC, Scheltens P, Barkhof F, Vrenken H. Whole-brain atrophy rate and cognitive decline: longitudinal MR study of memory clinic patients. Radiology. 2008; 248(2):590–8. 2482070938 [pii] 10.1148/radiol.2482070938 [doi]. [PubMed: 18574133]

Stavitsky K, Du Y, Seichepine D, Laudate TM, Beiser A, Seshadri S, Decarli C, Wolf PA, Au R. White matter hyperintensity and cognitive functioning in the racial and ethnic minority cohort of the Framingham Heart Study. Neuroepidemiology. 2010; 35(2):117–22. 000313443 [pii] 10.1159/000313443 [doi]. [PubMed: 20551699]

Thompson PM, Hayashi KM, De Zubicaray GI, Janke AL, Rose SE, Semple J, Hong MS, Herman DH, Gravano D, Doddrell DM, Toga AW. Mapping hippocampal and ventricular change in Alzheimer disease. Neuroimage. 2004; 22(4):1754–66. [PubMed: 15275931]

Wang L, Khan A, Csernansky JG, Fischl B, Miller MI, Morris JC, Beg MF. Fully-automated, multi-stage hippocampus mapping in very mild Alzheimer disease. Hippocampus. 2009; 19(6):541–8. 10.1002/hipo.20616 [doi]. [PubMed: 19405129]

Werft W, Benner A. glmperm: A Permutation of Regressor Residuals Test for Inference in Generalized Linear Models. The R Journal. 2010; 2(1):39–43.

Whitwell JL, Josephs KA, Murray ME, Kantarci K, Przybelski SA, Weigand SD, Vemuri P, Senjem ML, Parisi JE, Knopman DS, Boeve BF, Petersen RC, Dickson DW, Jack CR Jr. MRI correlates of neurofibrillary tangle pathology at autopsy: a voxel-based morphometry study. Neurology. 2008; 71(10):743–9. 71/10/743 [pii] 10.1212/01.wnl.0000324924.91351.7d [doi]. [PubMed: 18765650]

Wu CC, Chawla F, Games D, Rydel RE, Freedman S, Schenk D, Young WG, Morrison JH, Bloom FE. Selective vulnerability of dentate granule cells prior to amyloid deposition in PDAPP mice: digital morphometric analyses. Proc Natl Acad Sci U S A. 2004; 101(18):7141–6. 10.1073/pnas. 0402147101 0402147101 [pii]. [PubMed: 15118092]

Xie J, Alcantara D, Amenta N, Fletcher E, Martinez O, Persianinova M, DeCarli C, Carmichael O. Spatially localized hippocampal shape analysis in late-life cognitive decline. Hippocampus. 2009; 19(6):526–32. [PubMed: 19437501]

Abbreviations

CA	*Cornu Ammonis*
HP	Hippocampus
PCA	Principal Components Analysis
LoCA	Localized Components Analysis
ROI	Region of interest
PIB	Pittsburgh Compound B
ADNI	Alzheimer's Disease Neuroimaging Initiative
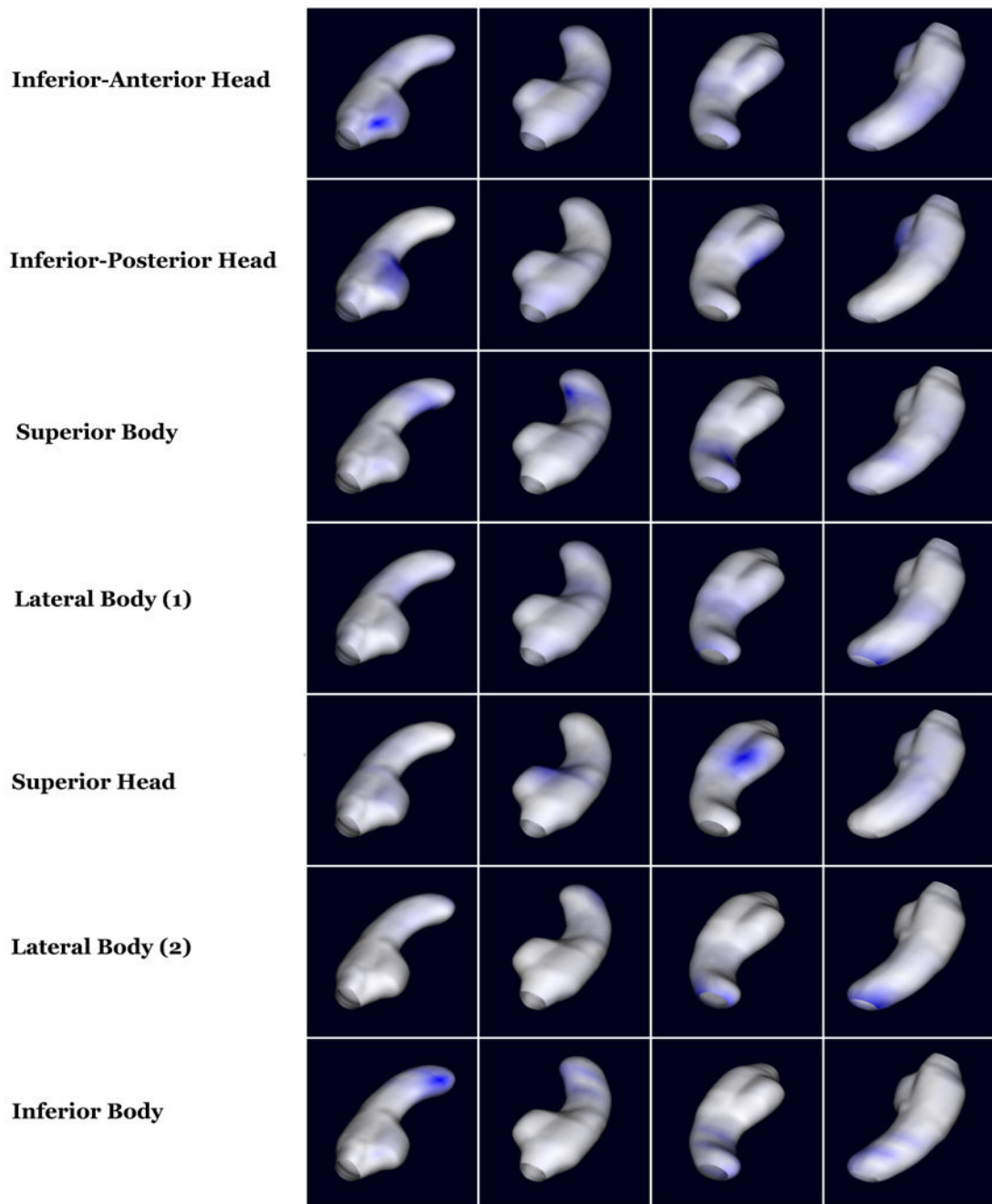
Figure 1.
Graphical depiction of the seven local hippocampus structural measures provided by LoCA.
Each row depicts a LoCA measure that describes atrophy to the hippocampal region shown
in blue. The first two oblique viewpoints show the inferior and superior aspects of the
population average hippocampus, with anterior (posterior) oriented toward the bottom (top)
of the image. The second two viewpoints show the medial-superior and lateral-inferior
aspects with anterior (posterior) oriented toward the top (bottom) of the image.
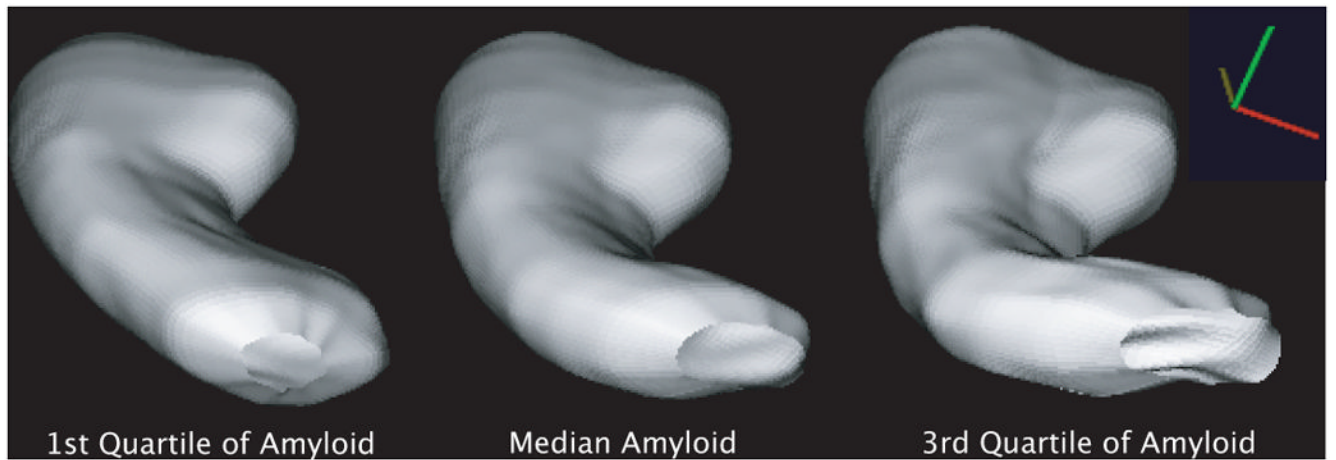
Figure 2.
Local hippocampus atrophy corresponding to a hypothetical cognitively-normal male subject whose age and total hippocampus volume were set to the cognitively-normal mean, and whose amyloid burden was set to the first quartile, median, and third quartile of cognitively normal participant values. See Results text for details. Red, yellow, and green axes correspond to medial, anterior, and superior directions respectively.
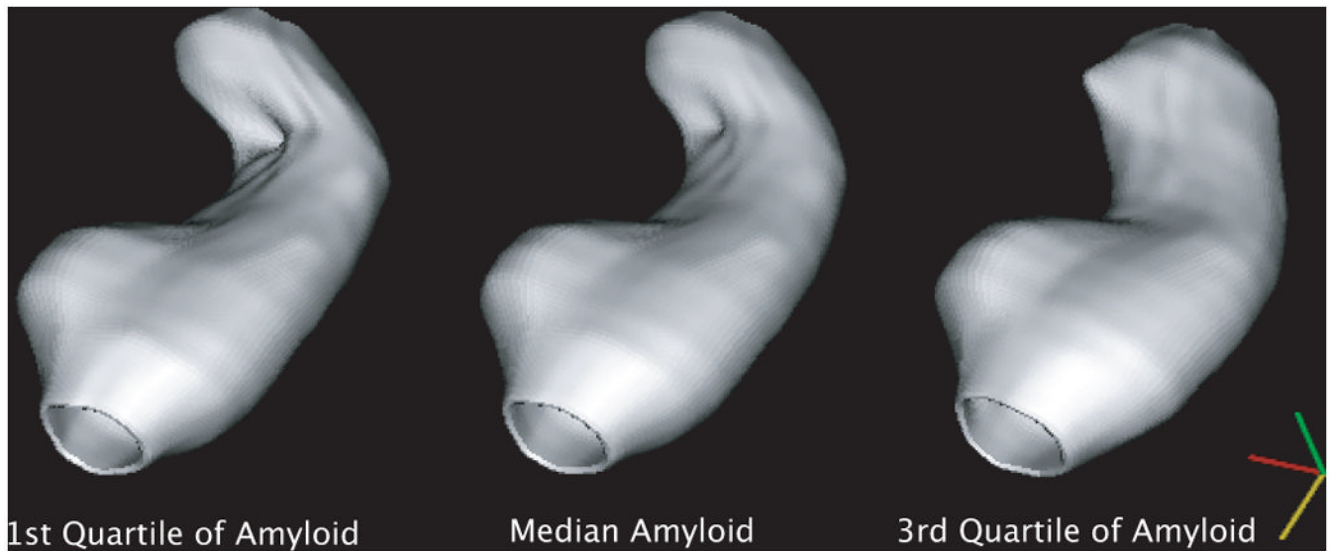
Figure 3.
Local hippocampus atrophy corresponding to a hypothetical male subject with MCI whose age and total hippocampus volume were set to the MCI mean, and whose amyloid burden was set to the first quartile, median, and third quartile of MCI participant values. See Results text for details. Red, yellow, and green axes correspond to medial, anterior, and superior directions respectively.

Figure 4.
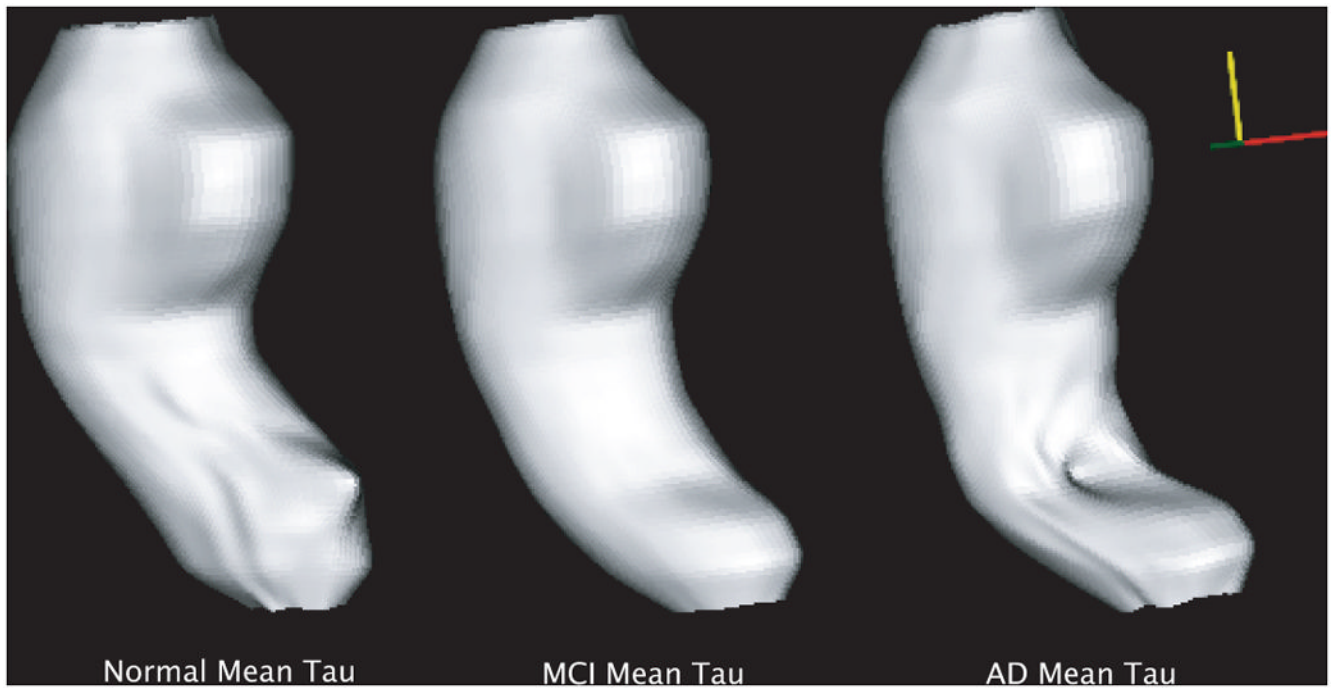Local hippocampus atrophy corresponding to a hypothetical male subject whose age and total hippocampus volume were set to the mean of the overall study population and whose tau burden was set to the mean values for normal, MCI, and AD participants. See Results text for details. Red, yellow, and green axes correspond to medial, anterior, and superior directions respectively.

Table 1

Subject characteristics

General characteristics of subjects who had MRI measures, and MRI and CSF measures, broken down by baseline clinical diagnosis. No differences between corresponding groups that had the same baseline clinical diagnosis but who had MRI, vs. both MRI and CSF, were significant at the *p*=.05 level. Superscript numbers indicate variables that differed significantly in t tests or chi squared tests at a p=.05 level between corresponding groups of baseline normal and baseline MCI [1], baseline normal and baseline AD [2], and baseline MCI and baseline AD [3] subjects. Italics indicate a group difference that was only significant between MRI groups.

Variable	Baseline-Normal		Baseline-MCI		Baseline-AD	
	With MRI	With MRI and CSF	With MRI	With MRI and CSF	With MRI	With MRI and CSF
Number of subjects	105	55	200	110	85	54
Age (mean +/− s.d.)	77.03 +/− 4.94	76.79 +/− 5.22	75.86 +/− 7.19	75.15 +/− 7.23	76.48 +/− 7.19	76.08 +/− 7.54
Years of education (mean +/− s.d.) [2]	16.01 +/− 2.76	15.69 +/− 3.03	15.74 +/− 3.02	15.65 +/− 3.12	15.07 +/− 3.15	15.44 +/− 3.24
Gender (# male; % male)	56; 53	29; 53	125; 62	71; 65	44; 52	30; 56
APOE genotype (% 2-3 or 2-4;3-3;3-4;4-4)	9.5; 64; 25; 1.9	15; 65; 20; 0	8; 40; 40; 13	6.4; 41; 37; 15	4.7; 28; 45; 22	3.7; 24; 44; 28
MMSE (mean +/− s.d.) [1,2,3]	29.3 +/− 0.75	29.33 +/− 0.77	27 +/− 1.8	27 +/− 1.8	23.26 +/− 1.8	23.26 +/− 1.9
ADAS-Cog (mean +/− s.d.) [1,2,3]	8.841 +/− 4.3	943 +/− 4.5	18.88 +/− 6.4	19.1 +/− 6.4	27.46 +/− 6.9	27 +/− 6.9
CDR Sum Of Boxes (mean +/− s.d.) [1,2,3]	0.05714 +/− 0.23	0.07273 +/− 0.26	3.18 +/− 1.8	3.145 +/− 1.8	8.306 +/− 3.1	8.315 +/− 3.1
Left HP Volume (mean *cc* +/− s.d.) [1,2,3]	2.1 +/− .31	2.1 +/− .29	1.8 +/− .36	1.78 +/− .34	1.58 +/− .35	1.57 +/− .36
Amyloid Beta 1-42 (mean *pg/ml* +/− s.d.) [1,2]		210 +/− 55		160 +/− 53		140 +/− 43
Total Tau (mean *pg/ml* +/− s.d.) [1,2,3]		72 +/− 32		100 +/− 46		120 +/− 57

Table 2

Associations between localized hippocampus atrophy and CSF amyloid

Permutation-corrected P values and regression coefficients for HP volume and localized atrophy measures as predictors of CSF amyloid. Values for volume are derived from multivariate regression models with age and gender as predictors. Values for localized atrophy measures are derived from multivariate regression models with age, gender, and HP volume as additional predictors. For P values less than .05, regression coefficients quantify the number of units of amyloid beta concentration decrease that were associated with a 1 *mm* decrease in local HP thickness in the localized HP region.

Diagnostic group	Hippocampal volume	Inferior Anterior Head	Superior Body	Inferior Body
Normal	0.759	**0.014, 11.5 *pg/ml***	**0.017, 9.9 *pg/ml***	**0.021, 12.4 *pg/ml***
MCI	0.438	0.465	**0.03, 6.18 *pg/ml***	0.44
AD	0.158	0.085	0.325	0.868

Table 3
Associations between localized hippocampus measures and cognition

Permutation-corrected P values and regression coefficients for the total HP volume and localized HP atrophy measures as predictors in multivariate statistical models of cognitive outcome measures. The hippocampal volume column shows values for models in which predictors were age, gender, and hippocampus volume. Other columns show values for models in which predictors were age, gender, hippocampus volume, and one of the localized atrophy measures. Regression coefficients are shown for $p<.05$, and these entries are shown in bold. For the localized atrophy measures, regression coefficients quantify the number of test score units decrease that were associated with a 1 *mm* decrease in local HP thickness in the localized HP region. For total HP volume, regression coefficients quantify the number of test score units decrease that were associated with a .1 cc decrease in HP volume.

Cognitive Variable	Hippocampal volume	Superior Body	Lateral Body (1)	Inferior Body
Animal Category	**<0.001, 0.39**	**0.042, 0.317**	**0.014, 0.515**	**0.046, 0.462**
Vegetable Category	**<0.001, 0.38**	**0.006, 0.283**	**0.029, 0.322**	**0.021, 0.375**
Digit Score	**<0.001, 0.701**	**0.001, 1.166**	**<0.001, 1.752**	0.363
AVLT Delayed	**<0.001, 0.38**	**0.007, 0.287**	0.529	**0.002, 0.544**
ADAS-Cog	**<0.001, −1.301**	**0.001, −0.788**	**0.009, −0.731**	**0.001, −1.043**
Trails A	0.147	**0.003, −1.606**	0.213	0.116
Trails B	**<0.001, −3.565**	**0.041, −2.893**	**<0.001, −7.01**	0.903
Immediate Story	**<0.001, 0.632**	**<0.001, 0.42**	0.112	0.064
Clock Score	**0.001, 0.608**	0.576	**0.001, 0.029**	0.758
Copy Score	**0.004, 0.01**	0.773	**0.029, 0.013**	0.723
Digit Span Forward	**0.002, 0.006**	0.38	0.123	0.533
Digit Span Backward	**0.002, 0.007**	0.907	**0.012, 0.025**	0.4
MMSE	**<0.001, 0.01**	**<0.001, 0.009**	**0.006, 0.008**	0.07
Boston Naming	**<0.001, 0.012**	0.216	0.658	**0.011, 0.017**
CDR Sum of Boxes	**<0.001, 0.011**	**<0.001, 0.096**	**0.01, 0.084**	**0.01, 0.094**
Delayed Story	**<0.001, −0.135**	**0.012, 0.051**	0.243	0.373